

# Lawrence Berkeley National Laboratory

## Lawrence Berkeley National Laboratory

### **Title**

PHOTOCATALYTIC AND PHOTOELECTROCHEMICAL HYDROGEN PRODUCTION ON STRONTIUM TITANATE SINGLE CRYSTALS

### **Permalink**

<https://escholarship.org/uc/item/72f8n0w6>

### **Author**

Wagner, F.T.

### **Publication Date**

2012-02-17



# Lawrence Berkeley Laboratory

UNIVERSITY OF CALIFORNIA

## Materials & Molecular Research Division

Submitted to the Journal of the American Chemical Society

PHOTOCATALYTIC AND PHOTOELECTROCHEMICAL HYDROGEN  
PRODUCTION ON STRONTIUM TITANATE SINGLE CRYSTALS

F. T. Wagner and G. A. Somorjai

April 1980

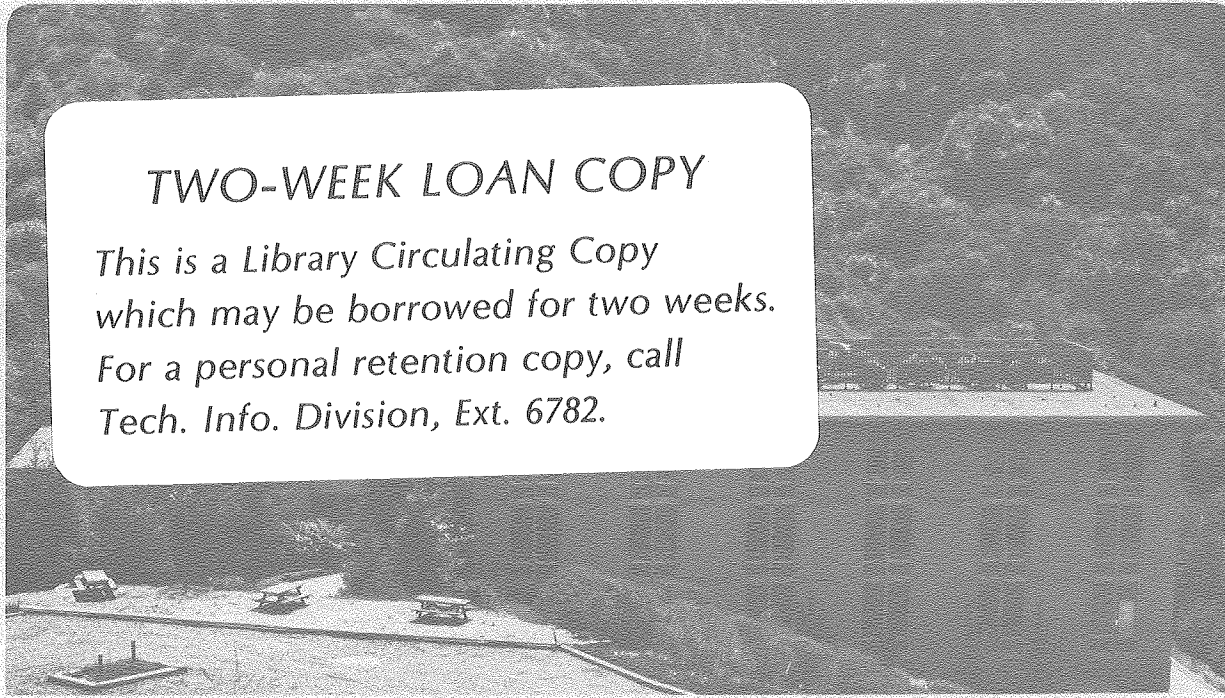
RECEIVED  
LAWRENCE  
BERKELEY LABORATORY

AUG 15 1980

LIBRARY AND  
DOCUMENTS SECTION

### TWO-WEEK LOAN COPY

*This is a Library Circulating Copy  
which may be borrowed for two weeks.  
For a personal retention copy, call  
Tech. Info. Division, Ext. 6782.*



LBL-10020 c. 2

## DISCLAIMER

This document was prepared as an account of work sponsored by the United States Government. While this document is believed to contain correct information, neither the United States Government nor any agency thereof, nor the Regents of the University of California, nor any of their employees, makes any warranty, express or implied, or assumes any legal responsibility for the accuracy, completeness, or usefulness of any information, apparatus, product, or process disclosed, or represents that its use would not infringe privately owned rights. Reference herein to any specific commercial product, process, or service by its trade name, trademark, manufacturer, or otherwise, does not necessarily constitute or imply its endorsement, recommendation, or favoring by the United States Government or any agency thereof, or the Regents of the University of California. The views and opinions of authors expressed herein do not necessarily state or reflect those of the United States Government or any agency thereof or the Regents of the University of California.

PHOTOCATALYTIC AND PHOTOELECTROCHEMICAL HYDROGEN  
PRODUCTION ON STRONTIUM TITANATE SINGLE CRYSTALS

F.T. Wagner and G.A. Somorjai

Materials and Molecular Research Division  
Lawrence Berkeley Laboratory and Department  
Of Chemistry, University of California  
Berkeley, CA 94720

Prepared for the U.S. Department of Energy  
under Contract W-7405-ENG-48



## Abstract

Sustained photogeneration of hydrogen was observed on metal-free as well as on platinized  $\text{SrTiO}_3$  single crystals illuminated in aqueous alkaline electrolytes or in the presence of electrolyte films. Hydrogen evolution rates increased with electrolyte hydroxide concentration, most strongly at hydroxide concentrations above 5N. Both stoichiometric and pre-reduced metal-free crystals were active for hydrogen photoproduction. No activity was observed from crystals in neutral or acidic solutions or in water vapor in the absence of a crust of a basic deliquescent compound. Metal-free crystals appear to evolve hydrogen via a photocatalytic mechanism in which all chemistry occurs at the illuminated surface. The results allow direct comparison of the photocatalytic and photoelectrochemical processes and have implications for the development of heterogeneous photocatalysis at the gas-solid interface.



## Introduction

The decomposition of water into hydrogen and oxygen using light energy absorbed by a semiconductor is one of the most promising means of converting solar energy into a storable fuel. The technological attractiveness of this reaction has drawn researchers to explore both photoelectrochemical and photocatalytic means of bringing it about. We use the term photocatalytic to describe processes, thermodynamically either uphill or downhill, in which both oxidation and reduction take place on a single illuminated catalytically active material. In photoelectrochemical reactions, on the other hand, the reduction and the oxidation of liquid or gas-phase species occur on different surfaces requiring net flows of charge between these surfaces in both the solid phase and the liquid or gas phase. We have measured both photoelectrochemical and photocatalytic hydrogen production from SrTiO<sub>3</sub> crystals illuminated in identical electrolytes. The rates for the two processes can thus be directly compared.

Ever since the initial publication on the photoassisted electrolysis of water by Fujishima and Honda,<sup>1</sup> considerable research has been directed towards the optimization of photoelectrochemical cells for this process. SrTiO<sub>3</sub>/Pt cells have been shown to efficiently photolyze water (up to a quantum yield for electron flow of 100% for  $\lambda < 3300\text{\AA}$ )<sup>2</sup> when illuminated by bandgap radiation.<sup>2,3,4</sup> In concentrated aqueous alkaline solutions these cells operate even at zero applied potential, though at reduced efficiency. Under these conditions, hydrogen yields of up to 16,000 monolayers per hour have been obtained.<sup>2</sup>

Photochemical diodes, which are in essence short-circuited electrochemical cells, have also proven effective in water photoelectrolysis.



Nozik<sup>5</sup> has shown that illumination of both sides of n-TiO<sub>2</sub>/GaP single crystal sandwiches in aqueous electrolyte yielded hydrogen and oxygen. Platinized n-SrTiO<sub>3</sub> single crystals<sup>6</sup> also split water when illuminated in aqueous alkaline electrolyte. In these photochemical diodes the exposed TiO<sub>2</sub> or SrTiO<sub>3</sub> surfaces served as photoanodes, while the GaP or Pt surfaces served as photoactive or passive cathodes.

The sustainable photoelectrolysis of water by liquid-phase photoelectrochemical cells and photochemical diodes is thus a well-established phenomenon. The sustained photocatalytic decomposition of water on semiconductors, however, has been on a less solid footing. Schrauzer and Guth<sup>7</sup> have reported the decomposition of chemisorbed water on illuminated TiO<sub>2</sub> powders. They observed hydrogen photoproduction up to the level of about one monolayer and proposed that a facile back-reaction prevented further hydrogen accumulation. Van Damme and Hall<sup>8</sup> illuminated TiO<sub>2</sub> in water vapor within a flow reactor to test the back-reaction hypothesis and detected no sustained hydrogen production. They proposed that a very slow rate of surface rehydroxylation has prevented sustained reactions at the water vapor TiO<sub>2</sub> interface.

We have observed sustained hydrogen photoproduction on both platinized and metal-free SrTiO<sub>3</sub> crystals illuminated in aqueous hydroxide solutions or in water vapor saturated films of NaOH or KOH. Hydrogen evolution from metal-free SrTiO<sub>3</sub> crystals appears to be photocatalytic rather than photoelectrochemical as it occurs on the illuminated surface of either pre-reduced or stoichiometric crystals. Platinized crystals produce hydrogen largely through the photoelectrochemical route. In both cases the rate of hydrogen production increases with increasing electrolyte hydroxide concentrations. No hydrogen production was detected from crystals illuminated in

neutral or acidic solutions or in room temperature water vapor when no crust of a basic deliquescent compound was present on the crystal surface<sup>8</sup>.

Our results indicate that a photocatalytic process in which both holes and electrons reach the illuminated SrTiO<sub>3</sub> surface can evolve hydrogen continuously from aqueous solution and that the hydroxide ion does play a role in the kinetics, in agreement with the proposals of Van Damme and Hall.

The experiments reported here were carried out in a vacuum cell batch reactor with a circulating gas phase composed of water vapor, argon and product gases. This gas was sampled periodically for chromatographic analysis. The apparatus is suitable for the study of gas-solid reactions (in which case the crystal can be cleaned and characterized under ultra-high vacuum conditions); liquid-solid reactions with the liquid in the form of a thin electrolyte film; or, with modifications, liquid-solid reactions in bulk liquid electrolyte of known concentration.

We are especially interested in the development of sustainable gas-solid photocatalytic reactions. Working in the gas phase enables one to independently vary partial pressures and temperature over wide ranges. This freedom may prove as useful in optimizing thermodynamic and kinetic parameters in photocatalytic processes as it has proven in standard heterogeneous catalysis. The techniques of modern surface science can be applied to the detailed characterization of catalysts employed in gas phase reactions. While progress in the application of such techniques to the study of reactions at the liquid-solid interface is being made, concentrated non-volatile electrolytes still pose great problems. By studying liquid-solid photoreactions in some depth, however, we hope to learn to increase the yield of analogous gas-phase reactions to allow more detailed studies of the relevant surface chemistry.

## Experimental Section

Crystal Preparation. The  $\text{SrTiO}_3$  wafers employed in this study were cut from single crystal boules supplied by National Lead and Commercial Crystal Laboratories. The boules were doped to about 100 ppm with tantalum. Spark-source mass spectroscopy kindly performed by Daniel Levy at Battelle Columbus Laboratories showed the following impurities: barium (10 ppm), iron (3.0 ppm), sulfur (1 ppm), and tantalum (>30 ppm).

Wafers approximately 1 mm thick were cut from the boules with a low-speed diamond saw. The wafers were oriented to within  $1^\circ$  of the (111) plane as determined by Laue back-reflection X-ray diffraction. Some crystals were polished to a mirror finish with  $1\mu$  diamond paste. Others, if properly oriented, were left with the finish imparted by the diamond saw or were ground with 600 grit SiC paper. Unpolished crystals gave similar hydrogen production rates to polished crystals, but gave superior platinum adhesion. Wafer frontal areas varied from 50 to 250  $\text{cm}^2$ .

"Pre-reduced" crystals were treated in flowing hydrogen at  $1000^\circ\text{C}$  for four hours. "Stoichiometric" crystals received no hydrogen or heat treatment. The back sides of "platinized" crystals were coated with metallic platinum by thermal decomposition of chloroplatinic acid. Electroplated and vacuum evaporated platinum coatings gave similar hydrogen production but poorer adhesion. Gold was deposited onto wafers by thermal decomposition of  $\text{AuCl}_3$ .

In some experiments one or more crystal faces were masked with Varian "Torr-seal" vacuum compatible epoxy. The epoxy darkened noticeably upon exposure to heat or ultraviolet light. However, the epoxy did not evolve hydrogen under our experimental conditions.

Reaction Cells. All experiments reported here were carried out in vacuum-line stirred batch reaction cells. Product detection was via chromatographic sampling of a circulating gas consisting of water vapor, argon and products. Two different reaction cells were used. In the first cell the gas phase circulated directly past the illuminated crystal, which was either clean or coated with a thin film of a soluble ionic compound. In the second, 'bulk liquid' cell the gas circulated over the surface of a 10 ml pool of electrolyte in which the illuminated crystal rested.

Figure 1a shows the experimental apparatus with the gas phase cell in use. The gas cell was mounted within a standard ultrahigh vacuum surface analytical chamber. When no added film of ionic compound coated the  $\text{SrTiO}_3$  crystal, it could be cleaned and analyzed under UHV conditions. The reaction cell was then closed around the crystal and water vapor was introduced from a glass bulb containing thoroughly outgassed ultrapure liquid water (Harleco 64112). All surfaces of the circulation loop could be thoroughly saturated with water by heating the glass bulb. The bulb was then valved off and the metal bellows circulation pump started. Pressure within the reactor loop was monitored with a capacitance manometer. The total volume of the loop was 170 ml.

Experiments in which the crystal was surrounded by a thin electrolyte film were also performed in the gas cell. The crystal and its vycor glass holder were dipped in a concentrated electrolyte solution. The resulting film was dried <sup>with</sup> hot air and the crystal mounted in the cell. The cell was then evacuated and back-filled with water vapor.

To explore the effects of film thickness, measured amounts of electrolyte solution could be spread over the crystal surfaces with a calibrated microliter pipette. The mean dry film thickness was then calculated using

the tabulated density of the ionic compound. Film thicknesses of basic compounds were confirmed by titration with HCl at the end of the experiment. The presence of the insulating film precluded the use of electron-beam surface analysis techniques.

The vacuum cell for carrying out reactions in bulk liquid electrolytes is shown in Figure 1b. The three-necked pyrex flask was inserted into the vacuum line in the place of the gas cell. Ground glass joints were sealed with Halocarbon 25-5S grease. The crystal rested on the bottom of the flask and was illuminated from below via a front-surface mirror. Several freeze-pump-thaw cycles served to outgas the electrolyte. Before sampling the gas phase, the flask was agitated to free bubbles from the crystal surface. The electrolyte temperature reached 44°C under illumination. The total volume of the circulation loop with the bulk liquid cell in place was 130 ml.

Product Detection. Product gases were separated and detected with a Hewlett-Packard 5720A Gas Chromatograph equipped with a thermal conductivity detector. An argon carrier gas and a molecular sieve 5A column were used. The gas chromatograph detector was calibrated by admitting gases into the reactor loop at low pressure and then sampling.

The minimum hydrogen production detectable at a signal-to-noise ratio of about 1:1 was  $1 \times 10^{16}$  molecules. The similar figure for oxygen is  $1 \times 10^{17}$  molecules and for nitrogen,  $2 \times 10^{17}$ . Detection of slow rates of oxygen

production proved problematic, with difficulties due to nonlinearities in gas chromatographic oxygen response and apparent adsorption effects.)

↪ Oxygen production rates greater than  $10^{17}$  molecules per hour were observable under ideal conditions. Air leaks into the reactor loop often precluded the detection of photogenerated oxygen.

After a number of experiments were carried out with  $\text{SrTiO}_3$  crystals coated with NaOH, the reactor loop itself began to evolve a small amount of hydrogen upon contact with water vapor. Direct application of NaOH to the stainless steel reaction cell walls caused no increase in background hydrogen. The background reactivity could be removed by rinsing the system with dilute nitric acid and copious amounts of distilled water. Because of this small background reactivity, blank runs in which no  $\text{SrTiO}_3$  was present, but where the NaOH-coated glass holder was in the cell, were frequently performed. The background rate was usually about  $3 \times 10^{15}$  molecules per hour. All data reported here were obtained under conditions where background hydrogen production was less than  $12 \times 10^{15}$  molecules per hour. In an analogous electrochemical cell this would correspond to a current of  $0.3 \mu\text{A}$ .

In this work hydrogen yields are described in terms of "monolayers" of hydrogen evolved. Looking down the [111] axis, the  $\text{SrTiO}_3$  structure consists of nearly closest-packed planes of stoichiometry  $\text{SrO}_3$  with Ti in octahedral holes between planes. There are  $1.14 \times 10^{15}$  oxygen atoms per  $\text{cm}^2$  in this closely packed (111) plane. To allow direct calculation of quantum yields, we define one monolayer as  $1 \times 10^{15}$  molecules  $\text{H}_2$  product per  $\text{cm}^2$  of illuminated cross sectional area. Since our crystals have illuminated areas of approximately  $1 \text{ cm}^2$ , one monolayer corresponds to about 2 nanomoles, and we can detect the presence of 10 monolayers

in the gas phase. To determine whether a given reaction is a catalytic or a surface stoichiometric process, the product yield should be normalized to the total surface area of the catalyst, since the entire surface could serve as a reservoir for an adsorbed species involved in a surface stoichiometric reaction. On our single-crystal catalysts the ratio of total surface area to illuminated cross section is small ( $\sim 4$ , including a roughness factor of  $\sqrt{2}$ ). In our experiments production of more than 4 "monolayers" of product is an indication of a catalytic rather than stoichiometric reaction. On powdered catalysts the ratio of total surface to illuminated cross section is much greater ( $10^3$ - $10^4$ ), and normalization of product yield to the former is required to judge whether or not a reaction is catalytic.

Light Source. The source of light for all experiments was a 500 W high-pressure Hg lamp. A 2cm water cell absorbed much of the infrared

radiation, and a fused quartz lens system cast an image of the arc on the SrTiO<sub>3</sub> crystal 15 inches away. The total irradiance at the crystal location as measured by an Eppley thermopile was 23 mW/cm<sup>2</sup>.

The spectral distribution of the lamp's output in the wavelength range 2200-6000Å was measured with a Heath EU-701 monochromator and a photomultiplier tube of response type S-5. 57% of the energy of the lamp in this region is in photons with energy greater than the bandgap of SrTiO<sub>3</sub> (3.2 eV). About half of these bandgap photons are in an emission peak centered around 3.4 eV ( $\lambda=3650\text{Å}$ ). The other half have photon energies exceeding 3.7 eV, chiefly in a series of emissions around 3.9 eV ( $3150\text{Å}$ ). The total flux of bandgap photons to the crystal was  $2 \times 10^{16} \text{ cm}^{-2} \text{ sec}^{-1}$ .

Colored glass filters were used to distinguish quantum from thermal effects; 96% of the energy transmitted through the Corning 7-51 (UV-pass) filter in the wavelength range 2200-6000Å (total irradiance at crystal 4 mW/cm<sup>2</sup>) was in photons with  $h\nu > 3.2 \text{ eV}$ . The higher energy component of the bandgap radiation was attenuated more strongly by the 7-51 filter than was the peak at 3.4 eV. The Corning 3-74 (visible pass) filter allowed an irradiance of 13 mW/cm<sup>2</sup> on the crystal. Less than 1% of the energy transmitted in the wavelength region 2200-6000Å was in photons with  $h\nu > 3.2 \text{ eV}$ . To test the crystal heating effects of the light, a thermocouple was wired into a crystal mounted within the gas reaction cell. The cell was evacuated and backfilled with water vapor at 20 torr. When only the water filter was used the crystal temperature reached 95°C upon illumination. Adding the UV-pass filter decreased the temperature to 32°C. Upon replacing the UV-pass with the visible-pass filter, the temperature rose to 65°C. With only the water filter in place, the bulk liquid cell operated at 44°C.





## Results

1. Platinized Crystals/ in Thin Electrolyte Films. We have measured hydrogen and oxygen production from pre-reduced, platinized SrTiO<sub>3</sub> single crystals coated with films of water-soluble ionic compounds. The coated crystals were placed in the gas reaction well and saturated with water vapor. Their platinum-free surfaces were then illuminated. Hydrogen production of up to 1580 monolayers per hour was observed from NaOH-coated crystals. No hydrogen production occurred in the dark or in the absence of water vapor. Platinized SrTiO<sub>3</sub> crystals not coated with a soluble ionic compound produced no measureable hydrogen when illuminated in room temperature water vapor. NaOH-coated, platinized platinum foil also produced no hydrogen above background when saturated with water vapor and illuminated. (Figure 6)

Table I summarizes results obtained with films of various compounds on platinized SrTiO<sub>3</sub>. Hydrogen production was observed only with films of compounds which were both basic and deliquescent. A deliquescent compound has an affinity for water sufficiently strong that its powder, when left in contact with moderately moist air, turns into a pool of aqueous solution. Non-basic deliquescent compounds such as CaCl<sub>2</sub> proved inactive for hydrogen production. In bulk liquid electrolytes, non-basic or weakly basic ( $[\text{OH}^-] < 10^{-5}\text{M}$ ) solutions with anions less prone to oxidation or specific surface interactions than chloride F<sup>-</sup>, ClO<sub>4</sub><sup>-</sup> also proved ineffective in promoting hydrogen production (Table II). Films of hygroscopic compounds which also pick up water from the air but in insufficient quantity to actually dissolve, proved inactive, even in the case of the base Na<sub>2</sub>CO<sub>3</sub>.

Figure 2 shows the dependence of hydrogen production on the average dry thickness of the NaOH film, as calculated from the known number of micro-moles of NaOH spread evenly over the surface. Hydrogen production decreases as the thickness of the NaOH film becomes smaller. The hydrogen production for the 2 $\mu$  film is indistinguishable from background hydrogen. Measured film

thicknesses greater than  $30\mu$  could not be reliably maintained on the crystal due to gravity flow upon saturation with water vapor. The data for Figure 2 were obtained in random order of NaOH thicknesses. The back of the crystal employed had been electroplated with platinum. The cutoff in hydrogen production at around  $2\mu$  NaOH thickness was also observed on crystals which had been platinized by vacuum evaporation of the metal and which showed higher overall hydrogen production activity.

Figure 3 shows hydrogen and oxygen photoproduction from a KOH-coated platinized  $\text{SrTiO}_3$  crystal saturated with water vapor. The observed deviation from  $\text{H}_2:\text{O}_2::2:1$  stoichiometry is within the uncertainty in the calibration of sensitivities for hydrogen and oxygen detection. The slow decline in hydrogen production rate seen in Figure 3 is due at least in part to the confirmed loss of NaOH from the crystal by gravity flow and splattering. Hydrogen production rates in bulk aqueous electrolyte could be maintained for tens of hours.

The crude wavelength response of the hydrogen production is demonstrated in Figure 4. The nature of the 'UV' (bandgap) and 'visible' (sub-bandgap) illumination has been described in the experimental section. The total radiant energy flux during 'visible' illumination exceeded that during 'UV' illumination. The observed drop in gas-phase hydrogen during visible illumination is therefore not due to hydrogen adsorption on cooling surfaces. The jumps in free hydrogen indicated by dashed lines can be ascribed to adsorption-desorption effects, as the pressure in the reactor loop increased or decreased 2 torr when the color filters were removed or inserted.

Platinization of part of the front of the  $\text{SrTiO}_3$  crystal, rather

than its back, also proved effective for rapid hydrogen production. When the platinized region was sealed off with epoxy, hydrogen production rates dropped to those observed from crystals completely devoid of metallic coating. Platinum foil in pressure contact with an otherwise metal-free pre-reduced  $\text{SrTiO}_3$  crystal caused a slight reduction in the rate of hydrogen photoproduction. Pt foil also seemed to decrease the rate obtained from platinized crystals.

2. Platinized Crystals in / Bulk Aqueous Electrolyte. Wrighton, Wolczanski and Ellis<sup>6</sup>

have reported photoelectrolysis of water on platinized reduced  $\text{SrTiO}_3$  crystals in alkaline aqueous solutions. Our experience with similar crystals in various aqueous electrolytes is summarized in Table II. In this short-circuited configuration, hydrogen is produced only in alkaline electrolytes, Figure 5 shows hydrogen photo production at  $44^\circ\text{C}$  from a platinized pre-reduced  $\text{SrTiO}_3$  crystal as a function of the concentration of the NaOH electrolyte. Below 5N the hydrogen production increases less than two-fold per decade increase in  $[\text{OH}^-]$ . Above 5N the dependence is much more striking. The data in Figure 5 were gathered in random order of concentration. The platinized crystal employed had been polished to a mirror finish on the (111) plane and metallized on the back by thermal decomposition of chloroplatinic acid.

Platinized pre-reduced crystals gave somewhat larger hydrogen yields when illuminated in 20N NaOH than in water vapor saturated films. The hydroxide concentration in such films was not measured. A comparison of results in bulk liquid electrolyte with those in NaOH films is given in Table III.

Platinized stoichiometric crystals illuminated in 19N NaOH produced hydrogen at a rate about 1/30th of that observed from platinized pre-reduced crystals. This is within a factor of 2 of the rate obtained from

metal-free stoichiometric crystals. A pre-reduced crystal coated with gold rather than platinum yielded hydrogen at about 1/10 the rate seen from the platinized crystals. Bubbles were seen coming off both the illuminated  $\text{SrTiO}_3$  surface and the non-illuminated gold surface.

3. Metal-Free Crystals. Sustained hydrogen production was observed from  $\text{SrTiO}_3$  single crystals illuminated in concentrated NaOH solutions or in water vapor saturated NaOH films even in the absence of any metallic coating. Both pre-reduced and stoichiometric crystals were active for hydrogen photo production. Rates of hydrogen evolution ranged from 20 to 100 monolayers per hour and could be sustained for at least 10 hours.

Figure 6 compares hydrogen production from platinized and metal-free pre-reduced  $\text{SrTiO}_3$  crystals. The crystals were coated with NaOH, saturated with water vapor and illuminated with the full water-filtered output of the 500W Hg lamp. No hydrogen was produced when a piece of platinized Pt foil was substituted for the crystal under identical experimental conditions.  $\alpha\text{-Al}_2\text{O}_3$  and ground glass blanks, given the same cleaning treatments as the  $\text{SrTiO}_3$  crystals, also yielded no hydrogen when illuminated in 20N aqueous NaOH, even when partially covered with epoxy.

Figure 7 shows that UV illumination, but not visible irradiation at higher total energy flux, causes hydrogen evolution from a stoichiometric metal-free crystal in 19N NaOH. No oxygen evolution was detected. However, the expected oxygen production rate concomitant with hydrogen production from water is beneath the detection limit for oxygen of the apparatus. Prolonged illumination of a clear stoichiometric crystal in concentrated NaOH solution caused a slight darkening of the illuminated area.

Gas bubbles were observed forming only on the illuminated surfaces

of metal-free crystals. The sensitivity of visual verification of gas production was enhanced by the low operating pressure of the reaction cell. Sudden jumps in the hydrogen concentration of the circulating gas phase occurred when large bubbles which has been trapped under the illuminated surface of the crystal were released by agitating the reaction flask. No reduction in hydrogen evolution rates ensued when the non-illuminated surfaces of either stoichiometric or metal-free crystals were sealed off with epoxy. Thus, it appears that the hydrogen was produced at the illuminated semiconductor surface.

Spectrophotometric analysis showed no soluble titanium in the 20 N electrolyte after more than 700 monolayers of hydrogen had been produced upon illuminating a platinum-free, stoichiometric crystal. The electrolyte was acidified to pH <2 with  $\text{HNO}_3$ ,  $\text{H}_2\text{O}_2$  added, and the absorbance around 410 nm scanned to check for the presence of a peroxotitanium complex.<sup>9</sup> No absorbance was seen with a sensitivity to  $10^{-3}$  O.D, which would correspond to about five monolayers soluble titanium produced. Extraction of the crystal with 1N  $\text{HNO}_3$  followed by addition of  $\text{H}_2\text{O}_2$  to the extract also yielded no absorbance at 410 nm, indicating that no multilayer of stable titanium peroxide insoluble in basic solution had formed as the oxidation product of the reaction.

To further test the reducing power of the illuminated  $\text{SrTiO}_3$  surface,  $\text{Cu(II)}$  in the form of  $\text{CuF}_2$  was added to the 19N NaOH electrolyte. Photodeposition of copper metal on both pre-reduced and stoichiometric  $\text{SrTiO}_3$  crystals was observed. In contrast to previous reports of copper photodeposition on pre-reduced  $\text{SrTiO}_3$ <sup>6</sup> and  $\text{TiO}_2$ <sup>6,10</sup>, the majority of the metallic copper was observed deposited on the illuminated surface.

The hydroxide concentration dependence of hydrogen production from a metal-free stoichiometric crystal is shown in Figure 8. The results roughly parallel those from platinized pre-reduced crystals except that no hydrogen production could be detected at hydroxide concentrations below 10N.

Platinization of the dark side and edges of a stoichiometric crystal yielded at most a two-fold increase in hydrogen production. Illumination of the platinized side of the stoichiometric crystal produced no hydrogen, although some lamplight could be seen through the rather dense Pt film.

The maximum rates of hydrogen production observed on stoichiometric and pre-reduced crystals with or without metal coatings are summarized in Table III. Results in both bulk aqueous electrolyte and in water vapor saturated NaOH films are listed.

4. Gas Phase Results. No hydrogen production was observed upon illumination of SrTiO<sub>3</sub> crystals in about 20 torr of water vapor at room temperature when no film of a basic deliquescent compound was present on the crystal. These experiments were performed both with and without platinum in contact with the crystal and with and without the UV-pass filter. Hydrogen production rates above 12 monolayers per hour could have been unambiguously measured. Rates above five monolayers per hour would have been noticed.

Experiments were performed with several SrTiO<sub>3</sub>/Pt configurations. The first experiments were carried out on a reduced SrTiO<sub>3</sub>(111) crystal mounted in pressure contact with a platinum foil clip. The exposed surfaces of both SrTiO<sub>3</sub> and platinum were cleaned by sputtering with argon ions, heating in 10<sup>-7</sup> torr of oxygen, and mild annealing (about 500°C) in ultrahigh vacuum. Auger electron spectroscopy showed carbon contamination on both exposed surfaces of about 1/10 monolayer. The reaction cell was then closed around the crystal, a saturation pressure of water vapor admitted, and illumination started. No hydrogen production could be measured. The cell was then pumped down and opened, leaving the crystal once again in high vacuum. Auger electron spectroscopy showed either no change in surface composition or a decrease in carbon contamination after the exposure to water vapor and light.

A SrTiO<sub>3</sub>(111) crystal annealed in vacuum at around 1200°C for 10 hours yielded a simple low energy electron diffraction pattern with a unit mesh consistent with unreconstructed termination of the bulk structure. Exposure to 1000 Langmuirs (1 Langmuir=10<sup>-6</sup> torr-sec) of H<sub>2</sub>O, O<sub>2</sub> or a mixture of H<sub>2</sub>O and NH<sub>3</sub> caused no diminution of LEED spot brightness or appearance of new spots. Heating the crystal to around 500°C in 10<sup>-6</sup> torr oxygen caused gradual disappearance of the LEED spots.





The water vapor experiments were repeated with crystals not cleaned in UHV. No hydrogen was observed from SrTiO<sub>3</sub>/Pt foil sandwiches or from platinized or metal-free pre-reduced crystals illuminated in 20 torr water vapor at room temperature in the absence of any film of soluble ionic compound. The same crystals gave sustained hydrogen yields in water-saturated NaOH films.

### Discussion.

Four main findings emerge from these results: (1) Sustained hydrogen and oxygen production occurs upon illumination of platinized pre-reduced SrTiO<sub>3</sub> crystals covered by water vapor saturated films of basic deliquescent ionic compounds. Similar rates of gas evolution were obtained in aqueous alkaline bulk liquid electrolytes. Gold coatings also accelerate hydrogen photoproduction on SrTiO<sub>3</sub>, but to a lesser extent than does platinum. (2) In the absence of any metal, but in the aqueous alkaline electrolyte or electrolyte film, sustained hydrogen production is observed from UV-illuminated SrTiO<sub>3</sub> crystals, either pre-reduced or stoichiometric. Both reduction and oxidation occur at the illuminated surface. (3) The rate of hydrogen production from both platinized and metal-free crystals increases with increasing concentration of the NaOH electrolyte. The dependence is weak below 5N but quite strong above that concentration. (4) No hydrogen production is observed when a SrTiO<sub>3</sub> crystal, either platinized or metal-free, is illuminated in pure water vapor at room temperature in the absence of any film of a soluble basic ionic compound. Each of these experimental findings will be discussed in turn.

1. Photoelectrochemical hydrogen production. Hydrogen production rates up to 4500 monolayers/hour were obtained from platinized pre-reduced SrTiO<sub>3</sub> crystals illuminated in 20N aqueous NaOH at 44°C. Roughly comparable

hydrogen photoproduction was obtained from such a photochemical diode coated with a thick ( $>30\mu$ ) crust of NaOH and saturated with water vapor. This similarity of rates, the need for thick NaOH films, the requirement of saturation water vapor pressures, and the need for deliquescent materials all argue for the equivalence of the experiments which were carried out in vapor-saturated films with experiments performed in bulk liquid electrolytes.

Wrighton, Wolczanski and Ellis<sup>6</sup> have observed hydrogen and oxygen photoproduction from platinized pre-reduced  $\text{SrTiO}_3$  crystals in aqueous alkaline solution. These photodiodes are thought to behave as short-circuited photo-electrochemical cells in which oxygen is produced at the illuminated bare  $\text{SrTiO}_3$  surfaces and hydrogen is evolved from the platinum-coated surfaces. Our results support the conclusion that this is the major mode of hydrogen photoproduction from platinized pre-reduced  $\text{SrTiO}_3$  crystals. When the platinized area of a pre-reduced  $\text{SrTiO}_3$  crystal was sealed off with epoxy, hydrogen production dropped to the level observed on metal-free crystals. Platinum foil in simple pressure contact with a metal-free pre-reduced  $\text{SrTiO}_3$  crystal did not accelerate hydrogen photoproduction; better contact between Pt and  $\text{SrTiO}_3$  was required. Platinization of the dark side of an insulating stoichiometric crystal increased its hydrogen photoproduction rate at most two-fold, whereas platinization of pre-reduced crystals of higher electrical conductivity increased hydrogen production up to seventy-fold. Thus if platinum is to have a marked catalytic effect in this process it must be in good electrical contact with a conducting  $\text{SrTiO}_3$  crystal. The major mode of hydrogen production on these photochemical diodes therefore appears to be electrochemical.

Coating the back surface of a pre-reduced  $\text{SrTiO}_3$  crystal with gold increased the rate of hydrogen photoproduction about seven-fold, around 1/10

the effect obtained with platinum (Table III). Kolthoff and Jordan<sup>11</sup> reported that hydrogen overpotentials for Au and Pt in 0.1N NaOH at a current density of  $18\mu\text{A}/\text{cm}^2$  (equivalent to the 200 monolayers  $\text{H}_2/\text{hr}$  we observed) were 380mV and 10mV, respectively. This difference in overpotentials is slightly greater than the reported difference between the flatband potentials of  $\text{TiO}_2$  and  $\text{SrTiO}_3$ .<sup>12</sup>  $\text{SrTiO}_3/\text{Au}$  would then be expected to evolve hydrogen more slowly than  $\text{TiO}_2/\text{Pt}$ . Recent measurements<sup>13</sup> have placed the true flatband potential of n- $\text{TiO}_2$  100mV negative of the  $\text{H}_2\text{O}/\text{H}_2$  couple, where hydrogen photogeneration on  $\text{TiO}_2/\text{Pt}$  would be thermodynamically possible.

The high quantum yields (up to 100% of photons absorbed)<sup>2</sup> attainable in photoelectrochemical reactions are in part due to two factors involving the spatial separation of oxidized and reduced species. The first is the efficient separation of photogenerated electrons and holes by the electric field within the semiconductor depletion layer. This separation inhibits electron-hole recombination and allows the mobile charge carriers produced by photons absorbed hundreds of Angstroms beneath the crystal surface to reach the interfaces with the electrolyte and carry out redox chemistry. This harvesting of light absorbed deep beneath the surface is of great importance to overall quantum efficiency since a monolayer of a material, even of one with a high absorption coefficient ( $10^5\text{cm}^{-1}$ ) can absorb only about 1% of the incident light of bandgap energy.

The second factor leading to high quantum yields in photoelectrochemical cells is the inhibition of back-reactions by the spatial separation of reductive and oxidative surface sites. The possible importance of back-reactions in the presence of platinum is shown in the 'dark' and 'visible' portions of Figure 4 and is further suggested by the observation that the

presence of platinum foil in pressure contact with a  $\text{SrTiO}_3$  crystal seemed to decrease the observed rate of hydrogen production. However, the reproducibility of this decrease of hydrogen partial pressure in the dark was poor.

While these two factors involving separation of reduced and oxidized species lead to high quantum yields, they also require a net flow of charge in the form of ions between the cathodic and anodic surfaces to complete the circuit started by the solid-state flow of electrons from anodic to cathodic surfaces. Although the photoelectrochemical process is highly efficient for reactions at the solid-aqueous electrolyte interface, it is unlikely to be efficient for reactions at the gas-solid interface since the gas phase cannot readily support such an ion current. The investigation of other surface photochemical mechanisms, even if they prove less efficient at the solid-liquid interface than the photoelectrochemical process, is thus of considerable interest. In the next section a photocatalytic process for hydrogen evolution which may not require long range ion transport will be discussed.

## 2. Photocatalytic Hydrogen Production.

We observed sustained hydrogen photoproduction from metal-free  $\text{SrTiO}_3$  crystals, either pre-reduced or stoichiometric, on the order of 20-100 monolayers/hour (Figure 6, Table III). This is 1/20 to 1/200 of the rates obtained on platinumized pre-reduced crystals. A highly concentrated (>5N) NaOH electrolyte or water vapor saturated NaOH film was required for measureable hydrogen production. The evolution of hydrogen could be maintained for tens of hours.

A number of photon-assisted reactions have been reported on oxide semiconductors with no metallic coatings. Both oxidations and reductions of solution species have been confirmed. Materials which have been oxidized on illuminated semiconductor powders include cyanide and sulfite<sup>14</sup>, rhodamine B<sup>15</sup>,

and acetic acid/acetate.<sup>1</sup> Several ions have been photoreduced to the metal on oxide semiconductor powders and/or single crystals:  $\text{Ag}^+$  17,18,  $\text{Au(III)}$  19,  $\text{Cu}^{2+}$  6,9,  $\text{Pd}^{2+}$  20,21, and  $\text{Pt(IV)}$  22. To our knowledge no / / unambiguously sustainable hydrogen photoproduction has been previously reported on platinum-free oxide semiconductors.

Hydrogen production from metal-free  $\text{SrTiO}_3$  appears to proceed via a photocatalytic, rather than photoelectrochemical, process in that all chemistry occurs on the illuminated surface. Gas evolution was visually confirmed only on the illuminated surface, and sealing off the non-illuminated surfaces of metal-free crystals, either pre-reduced or stoichiometric, caused no decrease in the rate of hydrogen evolution. The observation that stoichiometric and pre-reduced crystals evolved hydrogen at similar rates shows that good electrical conductivity is not a precondition for hydrogen evolution on metal-free crystals, thus giving further evidence against a simple analogy existing between this process and the operation of photoelectrochemical cells. This argument must be tempered by the observation that prolonged illumination (>24 hours) of stoichiometric crystals in concentrated aqueous NaOH caused a slight darkening of the otherwise clear crystals. This darkening is probably indicative of a slight reduction of the crystal. However, no detectable electrical conductivity could be obtained between probes on this darkened surface.

We have not measured oxygen photoproduction from metal-free crystals. However, the detection of oxygen production at rates concomitant with the hydrogen production observed on metal-free crystals would not be possible with our apparatus. The stoichiometry of the photoreaction on metal-free crystals thus remains to be determined--oxidized products other than  $\text{O}_2$  could be formed. The observations that the photoreaction took place on

stoichiometric as well as on pre-reduced crystals and that stoichiometric crystals darkened slightly upon illumination allows the inference that production of some gas or liquid phase oxidized product rather than net oxidation of the  $\text{SrTiO}_3$  crystal accompanies hydrogen production. The photoreaction on stoichiometric crystals demonstrates that the source of the hydrogen evolved from pre-reduced crystals was not the hydrogen used in crystal pre-treatment.

In  $\text{SrTiO}_3/\text{Pt}$  photoelectrochemical cells, conduction band electrons created by light absorption are driven away from the n-type  $\text{SrTiO}_3$  surface by the electric field within the semiconductor depletion layer. In the photocatalytic process described here, photogenerated electrons must reach the semiconductor surface to drive the observed reductive chemistry. A number of explanations, both within and without the band-bending model, can be brought forth to account for this phenomenon:

1. The driving force for hydrogen production on metal-free crystals may arise entirely from photons absorbed in the surface layer. Quantitative considerations bear out this possibility. The total flux of photons with energies greater than 3.2 eV under experimental conditions was about  $2 \times 10^{16} \text{ cm}^{-2} \text{ sec}^{-1}$ . About half of these photons were in a spectral peak around 3.4 eV; the other half were centered around 3.9 eV. Around room temperature the absorption coefficient  $\alpha$  for  $\text{SrTiO}_3$  is  $6 \times 10^3 \text{ cm}^{-1}$  at 3.4 eV<sup>23</sup> and  $3 \times 10^5 \text{ cm}^{-1}$  at a photon energy of 3.9 eV.<sup>24</sup> By use of these absorption coefficients one can calculate that 0.3% of the incident bandgap light would be absorbed within 2.26 Å of the surface. This is the distance between successive Sr-O closest packed (111) planes in  $\text{SrTiO}_3$ . This 0.3% of the incident light would lead to hydrogen production of 100 monolayers per hour, assuming 100%

quantum efficiency for photons absorbed in the surface layer. The observed hydrogen production rates were up to 100 monolayers per hour and were thus in a range consistent with effective photoexcitation in the surface layer only. The surface layer could be expected to exhibit different optical absorption properties than those found in the bulk. Low reaction rates precluded the measurement of the detailed wavelength dependence of hydrogen production from metal-free crystals, but insertion of a 7-51 color filter into the light beam caused a proportionately larger drop in hydrogen production on a metal-free stoichiometric crystal than on a platinized pre-reduced crystal. The 7-51 filter attenuates the higher energy photon intensity more strongly than it does the 3.4 eV peak. The larger drop in hydrogen production upon insertion of the filter should therefore be seen for the process more dependent upon photons absorbed near the surface. If bulk absorption coefficients are applicable, the photocatalytic process does then appear to rely on photons absorbed on the average nearer the surface than the average depth of photon absorption in the electrochemical process.

2. The observed photon-assisted reductive chemistry may be caused by photoelectrons created at depth and rising to the surface by an inefficient, essentially random-walk process. Such a process would be most effective in the absence of any appreciable band-bending. Even when a platinum counterelectrode is connected to the semiconductor, band-bending



is flattened by illumination. In the absence of any metal, this flattening could proceed still further as there would be no efficient process whereby electrons could leave the semiconductor bulk. With no appreciable band-bending present, both electrons and holes could diffuse to the surface, albeit with a high recombination rate.

3. If considerable band-bending were present, photo-generated electrons could be driven into the bulk until their energy equaled that of a surface acceptor state. They could then tunnel through the depletion layer barrier to the surface state where they would be available to reduce a solution species. Parkinson et al<sup>25</sup> have proposed such a shunting mechanism as an impediment to the efficient operation of GaAs liquid-junction solar cells, and Wrighton et al<sup>6</sup> have suggested that such a mechanism may be important to photocatalytic processes. However, a tunneling process would be very sensitive to the width of the band-bending barrier at the energy of the surface acceptor state. This width would be much greater for stoichiometric crystals with a low concentration of ionized donors than for heavily doped pre-reduced crystals. Yet stoichiometric and pre-reduced crystals exhibited similar rates of hydrogen photoproduction. It is possible that prolonged illumination reduced the near-surface regions of stoichiometric crystals so that near-surface doping levels for stoichiometric and pre-reduced crystals would be equivalent. In this case one would expect to see a definite induction period on stoichiometric but not on pre-reduced crystals if the tunneling mechanism were important. No such behavior was observed, although difficulties in dislodging small bubbles of hydrogen from the crystal surface made reliable studies with short time resolution at such slow rates of hydrogen production difficult.

The photocatalytic hydrogen production on metal-free  $\text{SrTiO}_3$  crystals occurs at 1/20 to 1/200 of the rate obtained via the photoelectrochemical process on platinized pre-reduced crystals. In the photocatalytic process all chemistry takes place on the illuminated  $\text{SrTiO}_3$  surface. / Since good electrical conductivity of the crystal is not required for photocatalytic hydrogen production, it seems likely that both oxidative and reductive surface chemistry take place not far from the point of photon absorption. The surface sites active for oxidation and reduction are likely to be interspersed on an atomic scale. Such a surface could be active for sustained gas-phase reactions, since no long-range ion transport through the gas phase would be necessary. However, no hydrogen production could be measured when  $\text{SrTiO}_3$  crystals, either metal-free or platinized, were illuminated in water vapor at around room temperature. The lack of hydrogen evolution from water vapor is not due solely to the lower number density of water molecules in the vapor than in the liquid (a factor of  $\sim 5 \times 10^4$ ) since no hydrogen evolution was observed in neutral or acidic aqueous electrolytes. The hydroxide concentration dependence of hydrogen photogeneration on  $\text{SrTiO}_3$  crystals to be discussed in the next section may give clues to kinetic barriers to photocatalytic water splitting at the gas-solid interface.

3. Hydroxide Concentration Dependence. The effects of changing the concentration of a sodium hydroxide electrolyte on hydrogen production from platinized and metal-free crystals are shown in Figures 5 and 8, respectively. On platinized crystals the concentration dependence of hydrogen photoproduction is weak in the concentration range  $10^{-3}$ -5N but becomes stronger above 5N. Roughly parallel behavior was observed on metal-free crystals

although no hydrogen photogeneration could be detected below 5N. No hydrogen evolution was seen in either case from neutral or acidic solutions (Tables I and II) or from pure water vapor at room temperature when no crust of a basic ionic compound was present. No definite cation effects were observed. The different rate observed with vapor saturated films of CsOH is believed to arise from the different water-absorbing properties of this compound relative to other alkali hydroxides. We will therefore describe the observed phenomenon simply as "hydroxide dependence", although the possible role of other bases has not yet been thoroughly explored.

The observed hydroxide dependence could arise from (1) direct participation of hydroxide in a rate-limiting step, (2) indirect kinetic control through an increase in band-bending associated with hydroxide adsorption, or (3) stabilization of new activated complexes or products in highly alkaline solutions. Our data and those of others provide some means of distinguishing between these possibilities.

Van Damme and Hall<sup>8</sup> have proposed that gas-solid "photocatalytic" reactions reported to date<sup>7,26</sup> have actually been stoichiometric reactions of surface hydroxyl groups; the reactions stop after all active surface hydroxyls have been consumed. The inability of water vapor to rehydroxylate the surface at reasonable rates may have prevented sustained photoreactions at the gas-solid interface. Boonstra and Mutsaers<sup>26</sup> reported photohydrogenation of acetylene on TiO<sub>2</sub> powders which stopped after the formation of a monolayer of products. Thermally dehydroxylated surfaces showed no photoactivity. Munuera et al<sup>27</sup> have correlated activity for the photodesorption of oxygen from TiO<sub>2</sub> powders with the presence of a particular surface hydroxyl species identified by means of infrared spectroscopy. They have shown that once these active

hydroxyls were destroyed by light they could not be regenerated by water vapor or liquid water at room temperature.<sup>28</sup> Harsher treatments were required. It thus seems possible that high electrolyte hydroxide concentrations are necessary to rapidly rehydroxylate at temperatures around 300°K the surface sites most active for hole transfer from the SrTiO<sub>3</sub>. Such a direct kinetic role for the hydroxide ion would account for the parallel hydroxide dependence observed on platinized and metal-free crystals with changing hydroxide concentration even though photogenerated charge carriers may be delivered to the active surfaces of these two types of crystals by quite disparate mechanisms with different sensitivities to changes in band-bending.

The increase in the strength of the hydroxide dependence above 5N is dramatic. A change in solvation state of the hydroxide ion, both in solution and, to a lesser extent, adsorbed on SrTiO<sub>3</sub>, could occur at these high concentrations. Kislina, et al<sup>29</sup> have employed infrared spectroscopy to study the solvation of hydroxide ions in 2.39-14.19N aqueous KOH. They have found that the mean hydration number for OH<sup>-</sup> decreases from 3 to 2 over this concentration range. Evidence for significant amounts of the proposed dihydrated hydroxide species first appears near 5N. Such a change in the actual chemical nature of the hydroxide ion could account for the discontinuous behavior of hydrogen photoproduction with increasing hydroxide concentration.

Bolts and Wrighton<sup>30</sup> have shown that, to the first order, changing the ambient pH in an electrochemical cell with a single homogeneous electrolyte has no effect on the thermodynamic relationships important to cell operation, including band-bending. This is true as long as the semiconductor flatband potential becomes more negative by 59 mV per unit increase in pH. They experimentally verified that this condition, which is an artifact of the

determination of surface net charge by simple  $H^+/OH^-$  equilibria, is satisfied by a number of oxide semiconductors, including  $SrTiO_3$ , over a pH range of 3 to 13. However, Mavroides et al<sup>3</sup> found that band-bending in  $SrTiO_3$  increased above pH 13, in the  $OH^-$  concentration regime where we have seen the strongest hydroxide dependence. Thus, the observed hydroxide dependence of the photoelectrochemical hydrogen production on platinized pre-reduced crystals could be explained by increased band-bending induced by specific adsorption of hydroxide ions. Such increased band-bending would decrease the rate of electron-hole recombination leading to more efficient hydrogen production. However, it is not clear how increased band-bending could increase the rate of photocatalytic hydrogen production on metal-free crystals unless photo-generated electrons reached the surface by tunneling through the band-bending barrier. As discussed earlier, such a tunneling mechanism seems unlikely in light of the similar rates of hydrogen production observed from stoichiometric and pre-reduced metal-free  $SrTiO_3$  crystals.

Although hydrogen photoproduction from platinized and metal-free  $SrTiO_3$  crystals shows a strong dependence on the electrolyte hydroxide concentration,  $SrTiO_3/Pt$  photoelectrochemical cells have been shown to operate efficiently in basic, neutral, or acidic media provided a sufficiently anodic potential is applied to the photoelectrode.<sup>2</sup> Wrighton et al<sup>2</sup> found no significant change in photocurrent for such a cell operated at 2.8 V applied potential over a hydroxide concentration range of 0.025-9.1N. Nasby and Quinn<sup>31</sup> have found that the photocurrent in a  $BaTiO_3/Pt$  cell operating at zero applied potential decreased with decreasing electrolyte pH. The effects of applied potential on the hydroxide dependence of photoelectrochemical hydrogen production may give clues as to the nature of this dependence.

An external anodic potential applied to an n-type SrTiO<sub>3</sub> photoelectrode appears largely across the semiconductor depletion layer, increasing the band-bending.<sup>3,2</sup> A high applied potential could cause sufficient band-bending to mask any changes in band-bending which might be induced by variation of the electrolyte hydroxide concentration. The effects of an external potential on surface hydroxyl concentration and the rate of surface hydroxylation is somewhat less clear. If essentially none of the applied potential appears across the inner Helmholtz layer, varying the applied potential should have minor, if any, effects on surface hydroxylation. It is also not clear how an applied potential could alter kinetics dependent upon the additional stabilization of new activated complexes or products with increased electrolyte hydroxide concentration.

Thus, no one of the simple explanations of the hydroxide dependence proposed here is consistent with all available data. A direct kinetic role for hydroxide agrees with all data at zero applied potential, but cannot explain the lack of hydroxide dependence in electrochemical cells at higher applied potential. An explanation based entirely upon induced band-bending deals successfully with the sensitivity of the hydroxide dependence to applied potential but cannot explain details of the experimental results obtained on metal-free crystals. The key to the kinetics of water splitting on illuminated semiconductor surfaces probably lies in the inhibition of electron-hole recombination. In photoelectrochemical cells operating at high applied potentials this inhibition is assured by the high electric field induced within the depletion layer by the applied potential. Most photogenerated electrons and holes are separated well within the bulk, and their recombination kinetics are not directly likely to be affected by surface chemical effects. The recombination lifetime

of electrons at the semiconductor surface is critical to the kinetics of photocatalytic reductions. This lifetime can be increased by the presence of hole-acceptor surface states which are themselves inefficient recombination centers.<sup>33</sup> Adsorbed hydroxide could form such surface states. The quantum efficiency for reduction would then increase with the surface hydroxide concentration which, under steady state conditions, depends on the rate of surface rehydroxylation. Hydroxide-induced band-bending and inhibition of recombination at the surface probably both play a role in the kinetics of photoelectrochemical cells operated at zero applied potential, where band-bending is marginal. Careful experiments in which light intensity, electrolyte pH, and (for electrochemical cells) applied potential are systematically varied, may be able to further elucidate the kinetic roles of hydroxide.

In summary, electrolyte hydroxide concentration has been found to be important to the rate of hydrogen photoproduction on platinized and metal-free  $\text{SrTiO}_3$  crystals. Hydroxide ions may be directly involved in a rate-limiting step, such as the production of active surface hydroxyl groups. Such an interpretation of our results in aqueous electrolyte is in agreement with reports that surface hydroxyl groups play a crucial role in semiconductor photochemistry at the gas-solid interface.<sup>8,26,27</sup>

4. Gas-Phase Considerations. We could measure no hydrogen production from platinized or metal-free  $\text{SrTiO}_3$  crystals illuminated in water vapor at a pressure of about 20t. Hydrogen production rates as low as twelve monolayers per hour could have been unequivocally detected. The same crystals coated with basic deliquescent compounds, saturated with water vapor, and illuminated yielded hydrogen at readily measureable rates.

Schrauzer and Guth<sup>7</sup> have reported the photodissociation of water on  $\text{TiO}_2$  powders. However, the process topped within several hours and could not be sustained to produce catalytic amounts of hydrogen. As discussed in the experimental section, product yields, to serve as a criterion for catalytic activity, should be normalized to the total surface area of the catalyst. Using the high end of their reported 0.5- $1\mu$  particle size range and assuming spherical particles, the maximum hydrogen accumulation they observed corresponded to  $\sim 2$  monolayers.

The ion-transport problems associated with photoelectrochemical reactions in the gas phase have already been discussed. We have, however, demonstrated that UV-illuminated metal-free  $\text{SrTiO}_3$  crystals in aqueous alkaline solution can evolve thousands of monolayers of hydrogen by a photocatalytic mechanism in which all chemistry occurs on the illuminated semiconductor surface. This finding lends support to the argument advanced by Van Damme and Hall<sup>8</sup> that some surface chemical problem, rather than problems with the delivery of photo-generated electrons and holes to the semiconductor surface, has restricted the yield of photoreactions at the gas-solid interface to one monolayer or less. The hydroxide dependence of the liquid phase photocatalytic reaction lends some support to their contention that the yield of the gas-phase reaction is limited by an inability to rehydroxylate the surface with water vapor. Development of techniques for the facile rehydroxylation of oxide semiconductor surfaces may prove a key to sustainable photocatalytic water dissociation at the gas-solid interface.

#### Acknowledgements.

This work was supported by the Division of Chemical Sciences, Office of Basic Energy Sciences, U.S. Department of Energy under Contract number W-7405-ENG-48.

F. T. W. was supported under an N. S. F. Graduate Fellowship.



References

1. Fujishima, A. and Honda, K., Bull. Chem. Soc. Jpn. 44, 1148 (1971).
2. M.S. Wrighton, A.B. Ellis, P.T. Wolczanski, D.L. Morse, H.B. Abrahamson and D.S. Ginley, J. Am. Chem. Soc. 98, 2774 (1976).
3. J.G. Mavroides, J.A. Kafalas, and D.F. Kolesar, Appl. Phys. Lett. 28, 241 (1976).
4. T. Watanabe, A. Fujishima and K. Honda, Bull. Chem. Soc. Jpn. 49, 355 (1976).
5. A.J. Nozik, Appl. Phys. Lett., 30, 567 (1977).
6. M.S. Wrighton, P.T. Wolczanski and A.B. Ellis, J. Solid State Chem. 22, 17(1977).
7. G.N. Schrauzer and T.D. Guth, J. Am. Chem. Soc. 99, 7189 (1977).
8. H. Van Damme and W.K. Hall, J. Am. Chem. Soc. 101, 4373, (1979).
9. J. Mühlebach, K. Müller, and G. Schwarzenback, Inorganic Chem. 9, 2381 (1970).
10. H. Reiche, W.W. Dunn and A.J. Bard, J. Phys. Chem. 83, 2248 (1979).
11. I.M. Kolthoff and J. Jordan, J. Am. Chem. Soc. 74, 4801 (1952).
12. M.A. Butler and D.S. Ginley, J. Electrochem. Soc. 125, 229 (1978).
13. M. Tomkiewicz, J. Electrochem. Soc. 126, 1505 (1979).
14. N. Frank and A.J. Bard, J. Phys. Chem. 81, 1484 (1977).
15. T. Watanabe, T. Takizawa and K. Honda, J. Phys. Chem. 81, 1845 (1977).
16. B. Kraeutler and A.J. Bard, J. Am. Chem. Soc. 100, 5985 (1978).
17. E. Bauer and A. Perrett, Helv. Chim. Acta 7, 919 (1924).
18. H. Jonker, C.J. Dippel, J.H. Houtman, C.J.G.F. Janssen and L.K.H. van Beek, Phot. Sci. Eng. 13, 1 (1969).
19. A.K. Bhattacharya and N.R. Phar, J. Indian Chem. Soc. 4, 299 (1926).
20. H. Jonker, C.J.G.F. Janssen, C.J. Dippel, T.P.G.W. Thijssens and L. Postma, Phot. Sci. Eng. 13, 45 (1969).
21. F. Möllers, H.J. Tolle and R. Memming, J. Electrochem. Soc. 121, 1160 (1974).
22. B. Kraeutler and A.J. Bard, J. Am. Chem. Soc. 100, 4317 (1978).
23. D. Redfield and W.J. Burke, Phys. Rev. B, 6, 3104 (1972).
24. M. Cardona, Phys. Rev. 140, A651 (1965).
25. B.A. Parkinson, A. Heller and B. Miller, J. Electrochem. Soc. 126, 954 (1979).
26. A.H. Boonstra and C.A.H.A. Mutsaers, J. Phys. Chem. 79, 2025 (1975).
27. G. Munuera, V. Rives-Arnau and A. Saucedo, J. Chem. Soc. Faraday Trans. I, 75, 736 (1979).
28. G. Munuera, op.cit., and personal communication.
29. I.S. Kislina, V.D. Maiorov, H.D. Librovich, M.I. Vinnik, Zh. Fiz. Khim. 50, 2812 (1976).

30. J.M. Bolts and M.S. Wrighton, *J. Phys. Chem.* 80, 2641 (1976).
31. R.D. Nasby and R.K. Quinn, *Mat. Res. Bull.* 11, 985 (1976).
32. A.J. Nozik, *Annu. Rev. Phys. Chem.* 29, 189 (1978).
33. P. Vohl, *Phot. Sci. Eng.* 13, 120 (1969).

Table Captions

- TABLE I. The hydrogen photoproduction activity of water vapor saturated ionic compound films on a platinized, pre-reduced  $\text{SrTiO}_3$ (111) crystal.
- TABLE II. Activity of aqueous electrolytes for hydrogen photoproduction on a platinized, pre-reduced crystal.
- TABLE III. Maximum rates of hydrogen photoproduction observed on  $\text{SrTiO}_3$  crystals (A) in NaOH films saturated with water vapor, (B) in 20N aqueous NaOH at  $44^\circ\text{C}$ .

TABLE I

	H <sub>2</sub> produced	no H <sub>2</sub> produced
NaOH, d	X	
KOH, d	X	
CsOH, d	X(1/2)	
CsCl, h		X
CaCl, h		X
LiCl, d		X
CaCl <sub>2</sub> , d		X
Na <sub>2</sub> CO <sub>3</sub> , h		X
Cs <sub>2</sub> CO <sub>3</sub> , d	X(1/2)	

d = deliquescent

h = hygroscopic, but not deliquescent

(1/2) = hydrogen evolved at about 1/2 the rate observed for NaOH.

TABLE II

<u>Electrolyte</u>	<u>H<sub>2</sub> produced</u>	<u>H<sub>2</sub> not produced</u>
.001-20N NaOH	X	
1-10N HClO <sub>4</sub>		X
10N H <sub>2</sub> SO <sub>4</sub>		X
1N NaClO <sub>4</sub>		X
1N NaF		X
10N LiCl		X
18N NH <sub>3</sub>	X	

TABLE III

- A. Hydrogen production from  $\text{SrTiO}_3$  crystals covered by thick ( $>30\mu$ ) NaOH films saturated with water vapor.

<u>Crystal</u>	<u>Monolayers† H<sub>2</sub>/hr</u>
Pre-reduced, platinized	1580
Pre-reduced, metal-free	100
Stoichiometric, metal-free	30

- B. Hydrogen production from  $\text{SrTiO}_3$  crystals in 20 M NaOH.

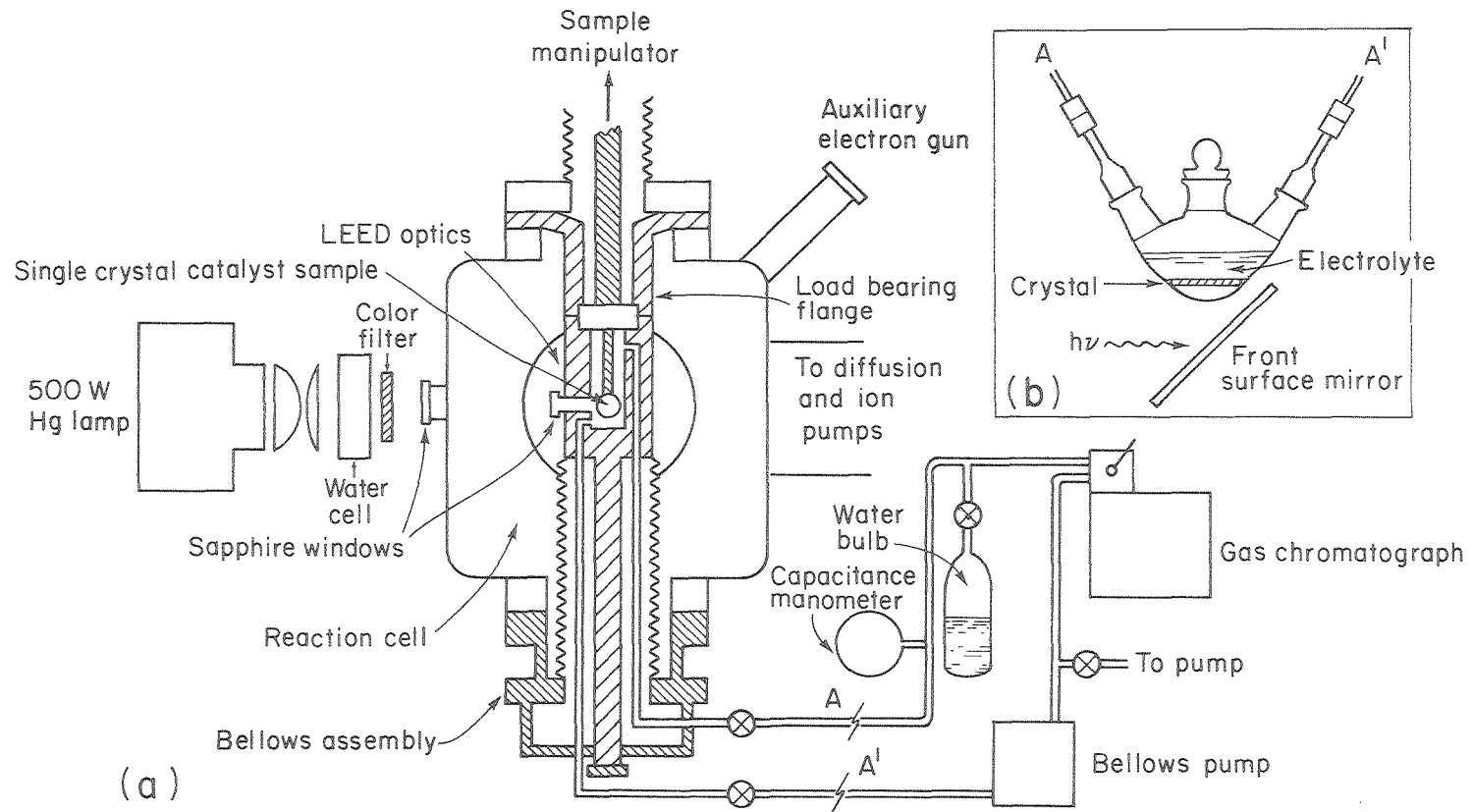
<u>Crystal</u>	<u>Monolayer † H<sub>2</sub>/hr</u>
Pre-reduced, platinized	4500
Stoichiometric, platinized	120
Pre-reduced, metal-free	30
Stoichiometric, metal-free	50
Pre-reduced, gold coated	200

†monolayer  $\equiv 1 \times 10^{15}$  molecules/cm<sup>2</sup> illuminated surface

Figure Captions

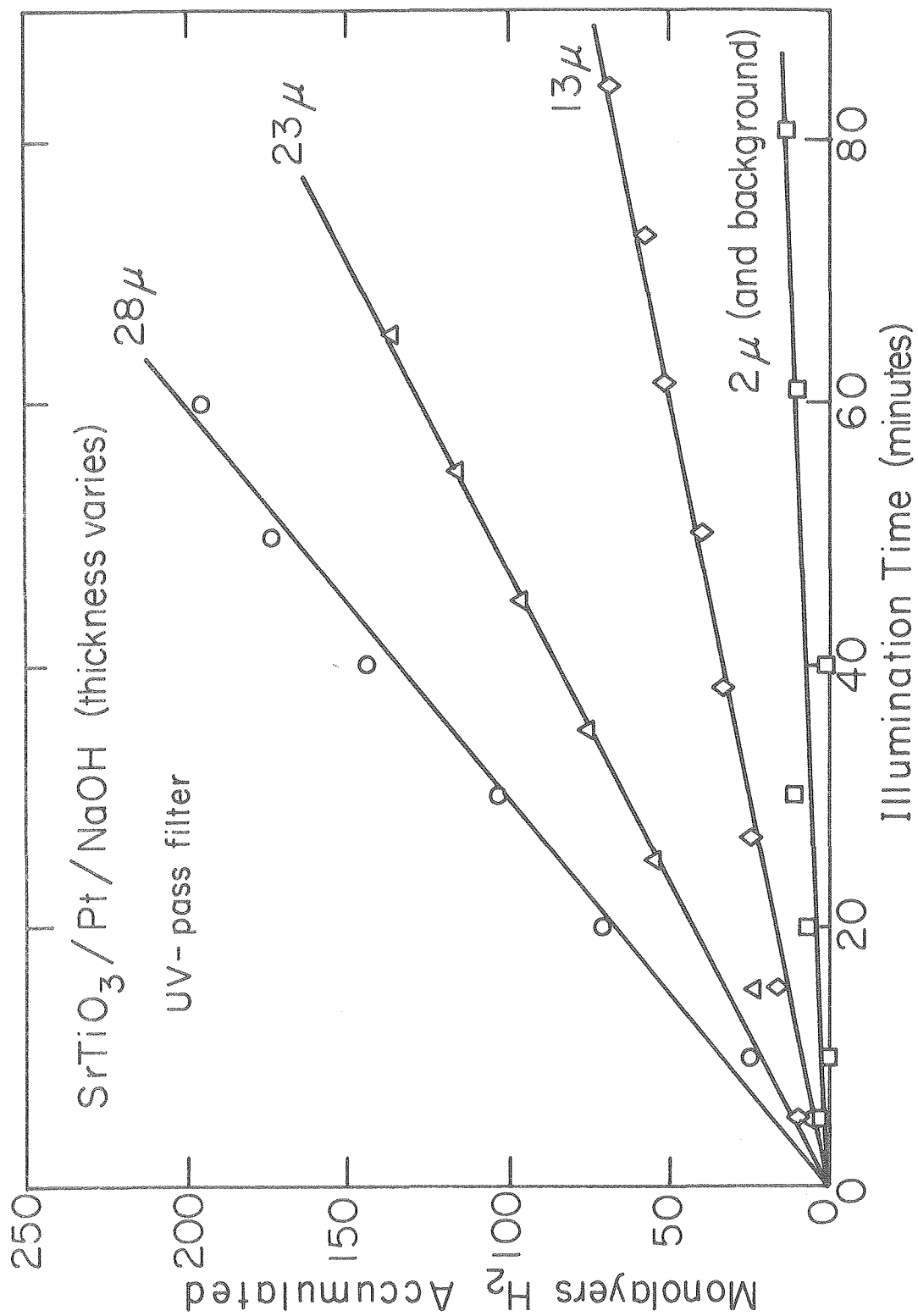
- Figure 1. Experimental apparatus. (a) Closed circulation loop including gas phase reaction cell within UHV chamber, (b) Reaction cell for studies in bulk liquid electrolytes, which replaces the gas phase reactor by attachment at points A and A'.
- Figure 2. Hydrogen photoproduction from a platinized n-SrTiO<sub>3</sub>(111) crystal coated with NaOH to varying thicknesses, saturated with water vapor and illuminated through a Corning 7-51 filter.
- Figure 3. Hydrogen and oxygen photoproduction from a platinized n-SrTiO<sub>3</sub> crystal encrusted with KOH, saturated with water vapor and illuminated with the full output of the 500W Hg lamp.
- Figure 4. Coarse wavelength dependence of hydrogen photogeneration on a platinized SrTiO<sub>3</sub> crystal coated with a 28μ layer of NaOH and saturated with water vapor. Light source: 500W Hg lamp. 'UV'= light passed by 2cm H<sub>2</sub>O and a Corning 7-51 filter. 'visible'= water and 3-74 filters. 'UV+Visible'=water filter only.
- Figure 5. Rate of hydrogen photoproduction on a platinized pre-reduced SrTiO<sub>3</sub>(111) crystal as a function of concentration of the aqueous NaOH electrolyte at 44°C. Light source: full output of 500W Hg lamp. Approximate scatter in data from other runs: +35%.
- Figure 6. Comparison of hydrogen photoproduction from pre-reduced platinized (□) and metal-free (○) SrTiO<sub>3</sub> crystals and a platinized platinum foil blank (Δ). Each was supported in a vycor glass holder, encased in NaOH, saturated with water vapor, and illuminated with the full output of the 500W Hg lamp.
- Figure 7. Hydrogen production from a stoichiometric, metal-free SrTiO<sub>3</sub>(111) crystal in 19N NaOH under visible (3-74 filter, 13mWcm<sup>-2</sup>) and UV (7-51 filter, 4mWcm<sup>-2</sup>) irradiation.
- Figure 8. Hydrogen photoproduction at 44°C on a stoichiometric, metal-free SrTiO<sub>3</sub>(111) crystal as a function of electrolyte NaOH concentration. Illumination: Full output of 500W Hg lamp (23mWcm<sup>-2</sup>).

Fig. 1



XBL7910-4558





XBL 799-7070

Fig. 2

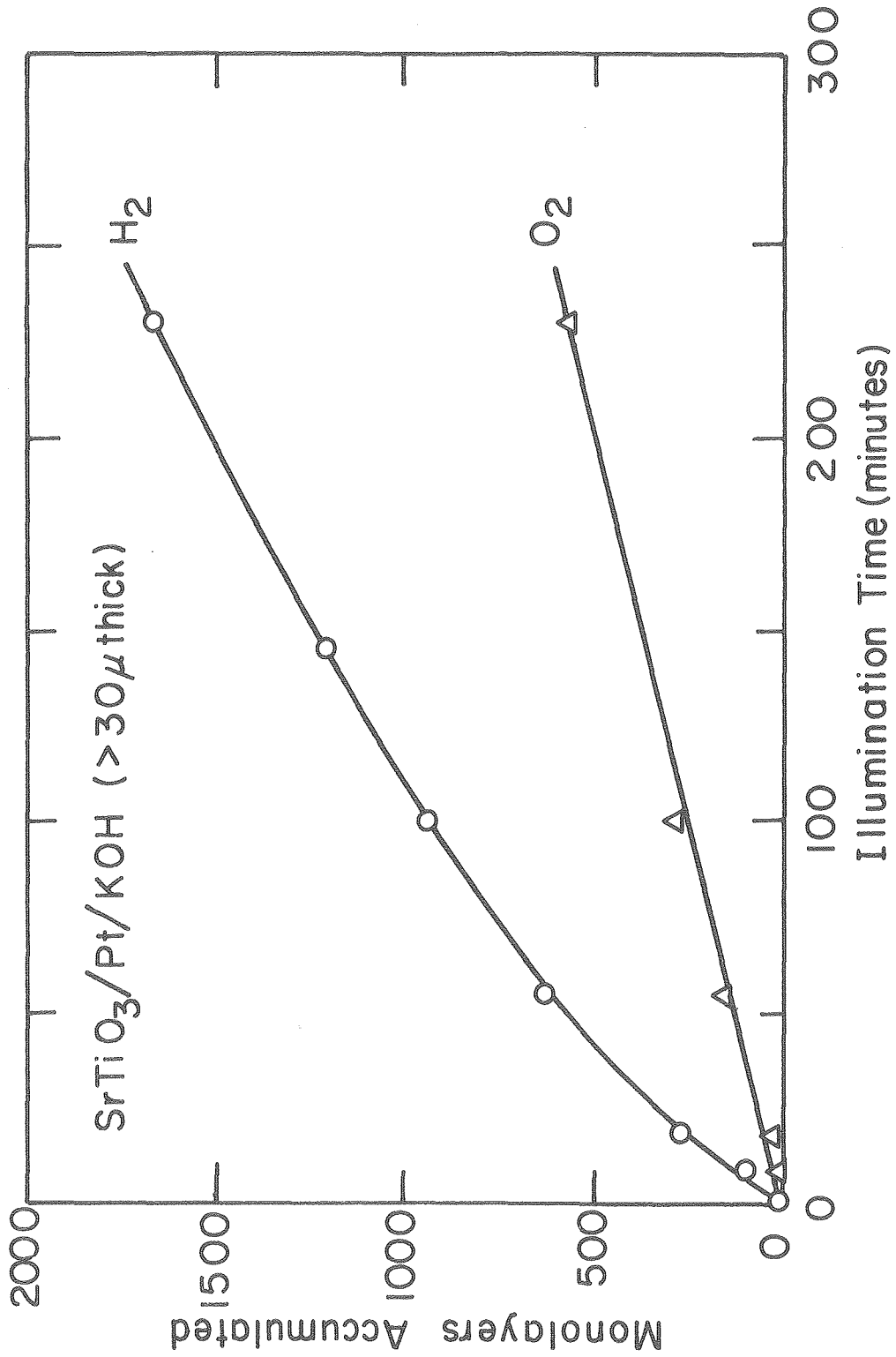


Fig. 3

XBL 799-7069

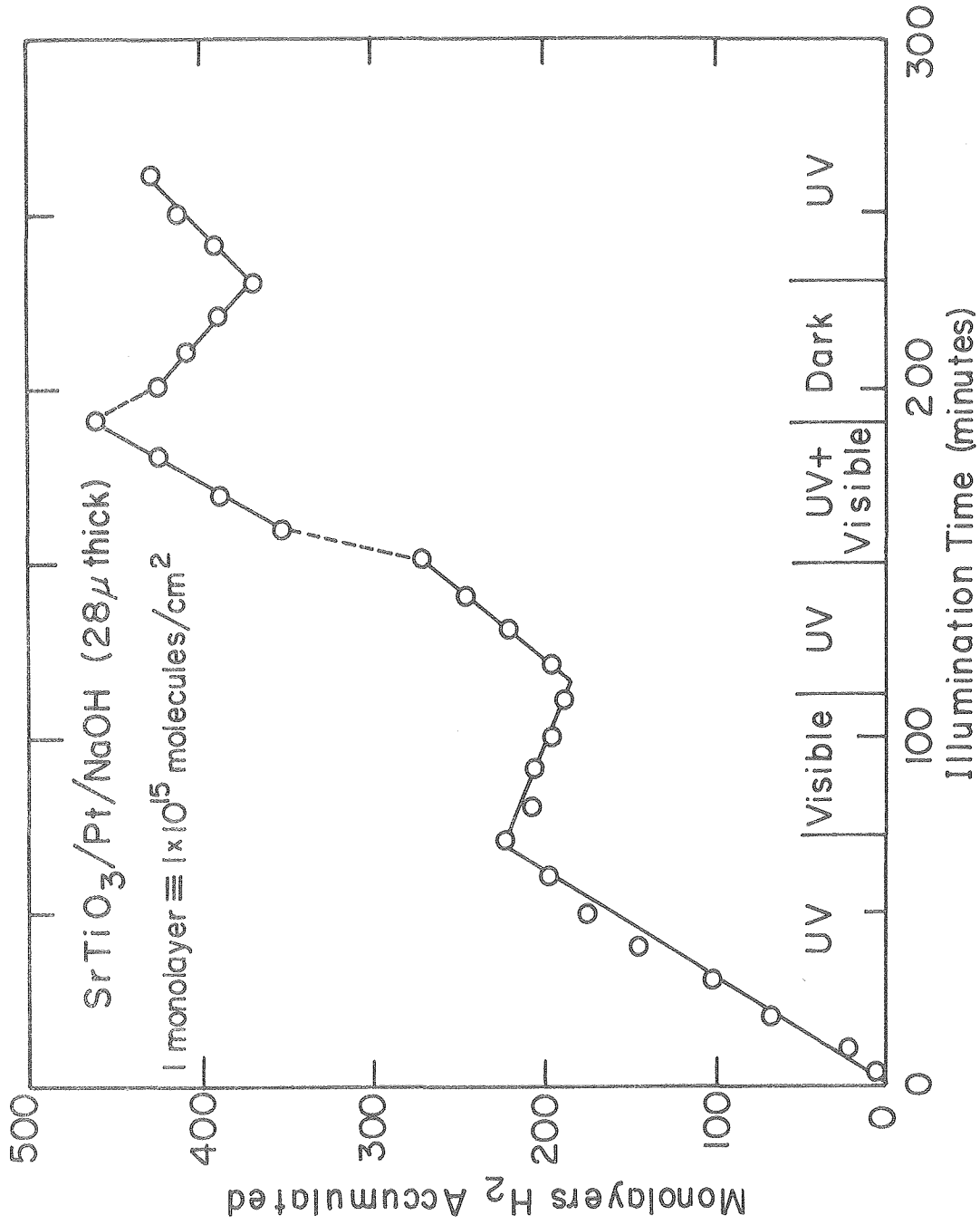
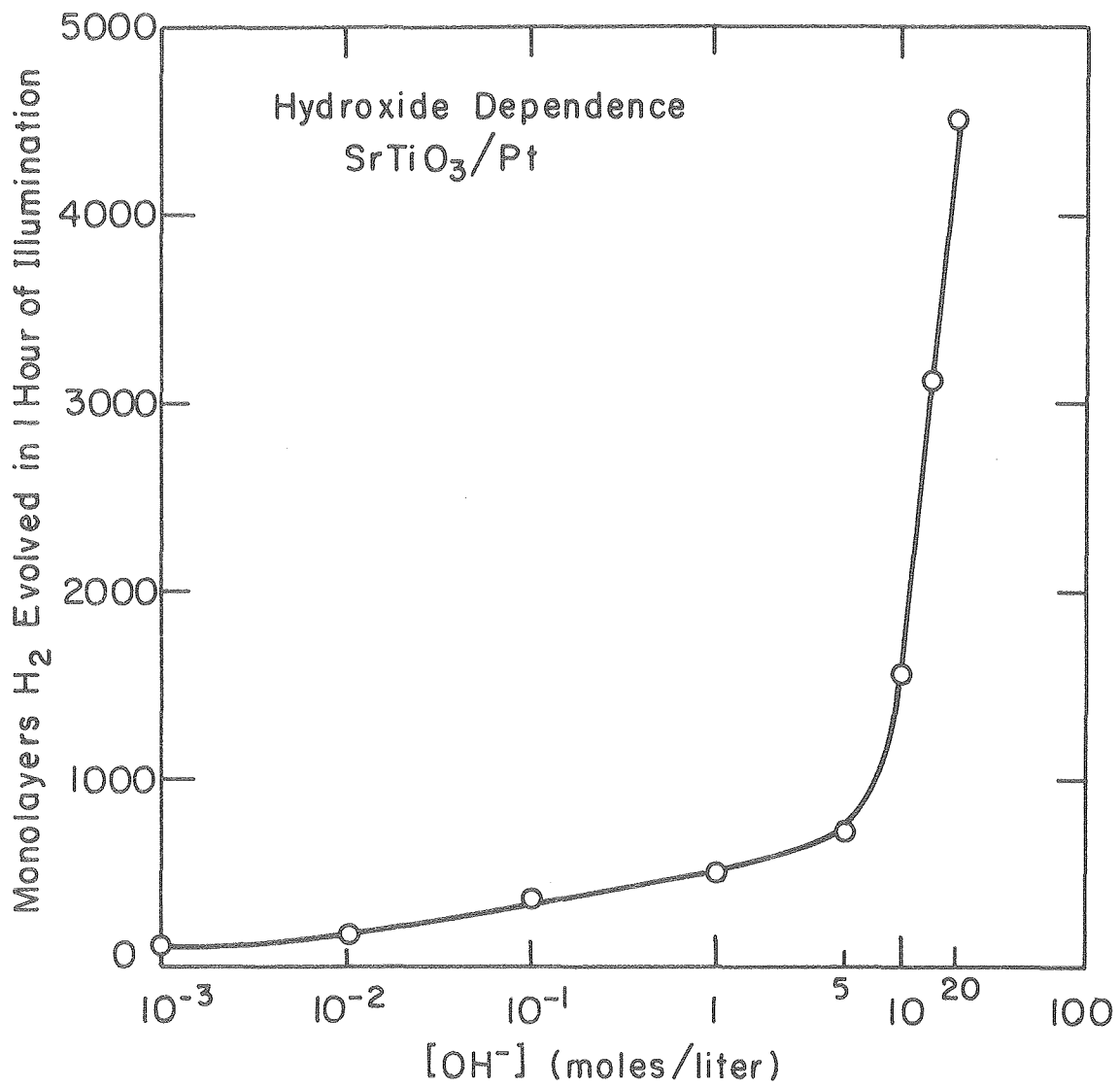


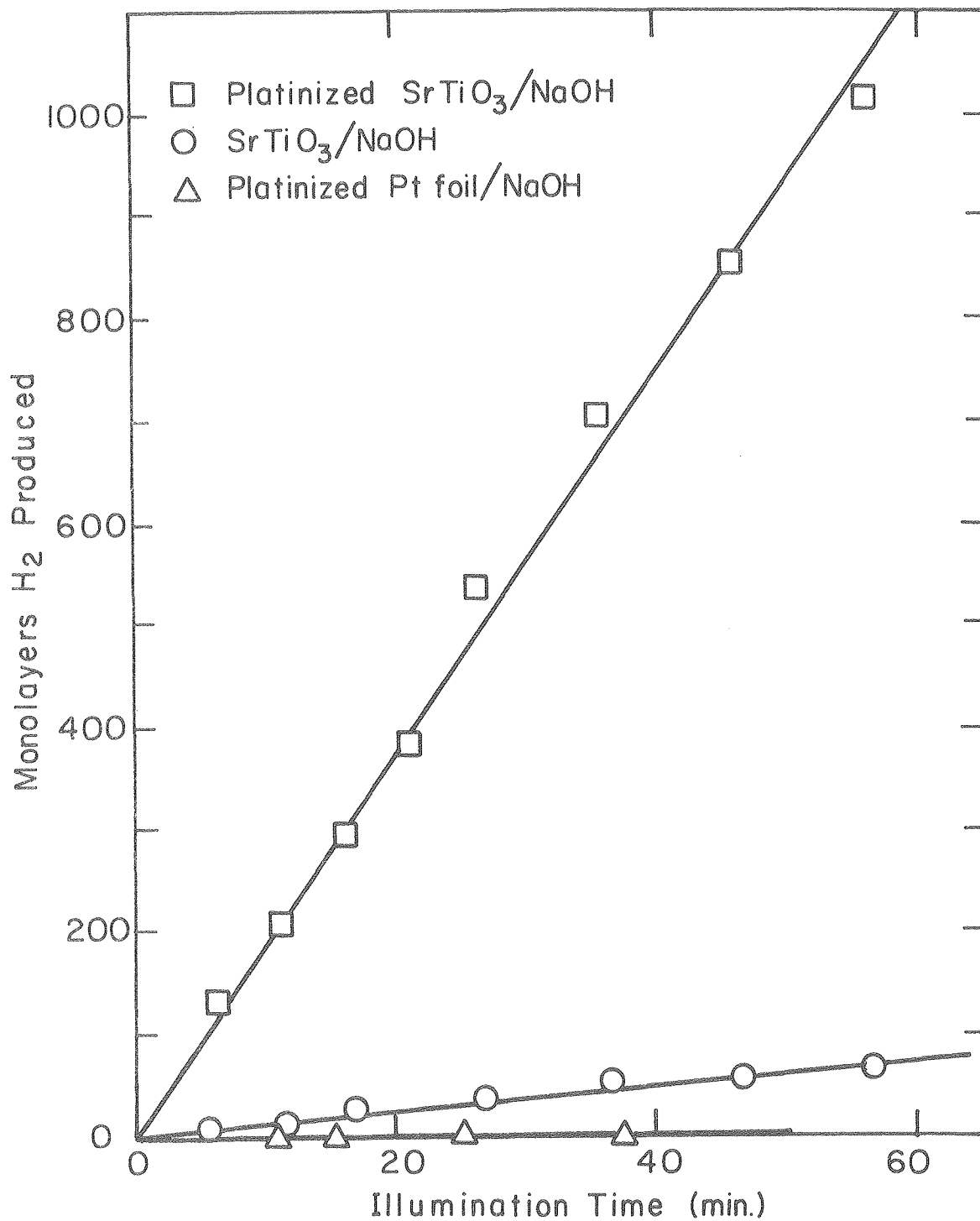
Fig. 4

XBL 799-7067



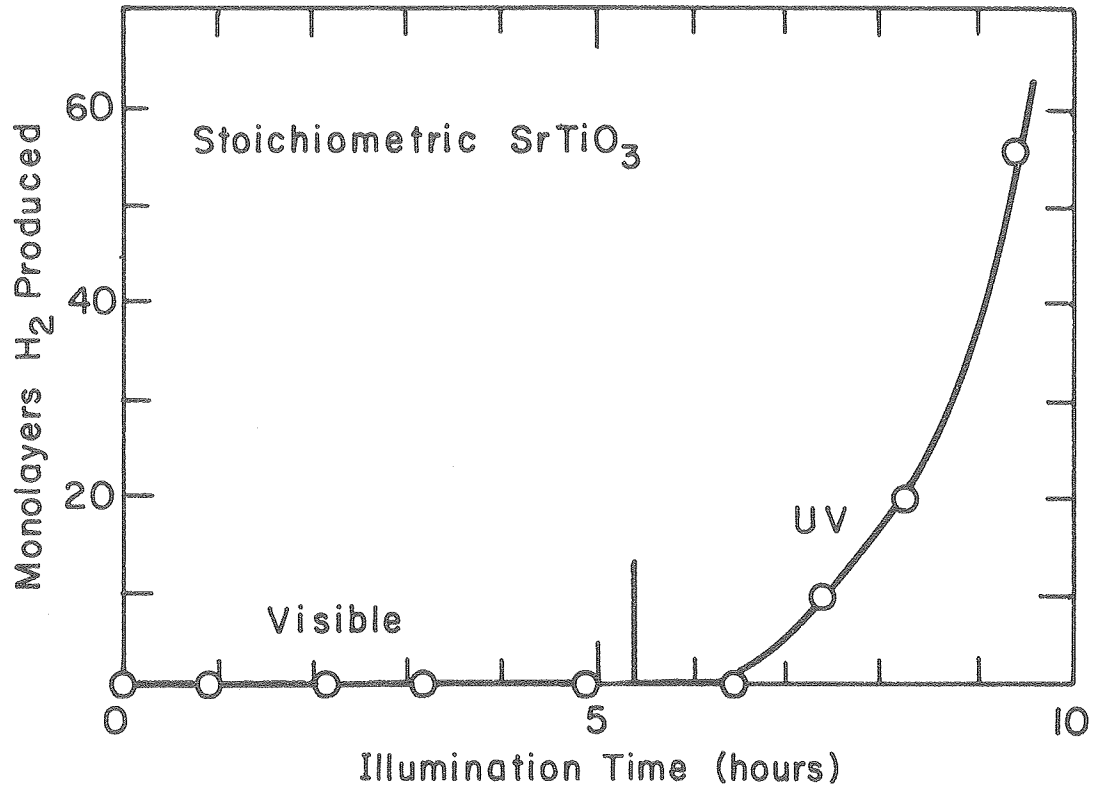
XBL799-7068

Fig.5



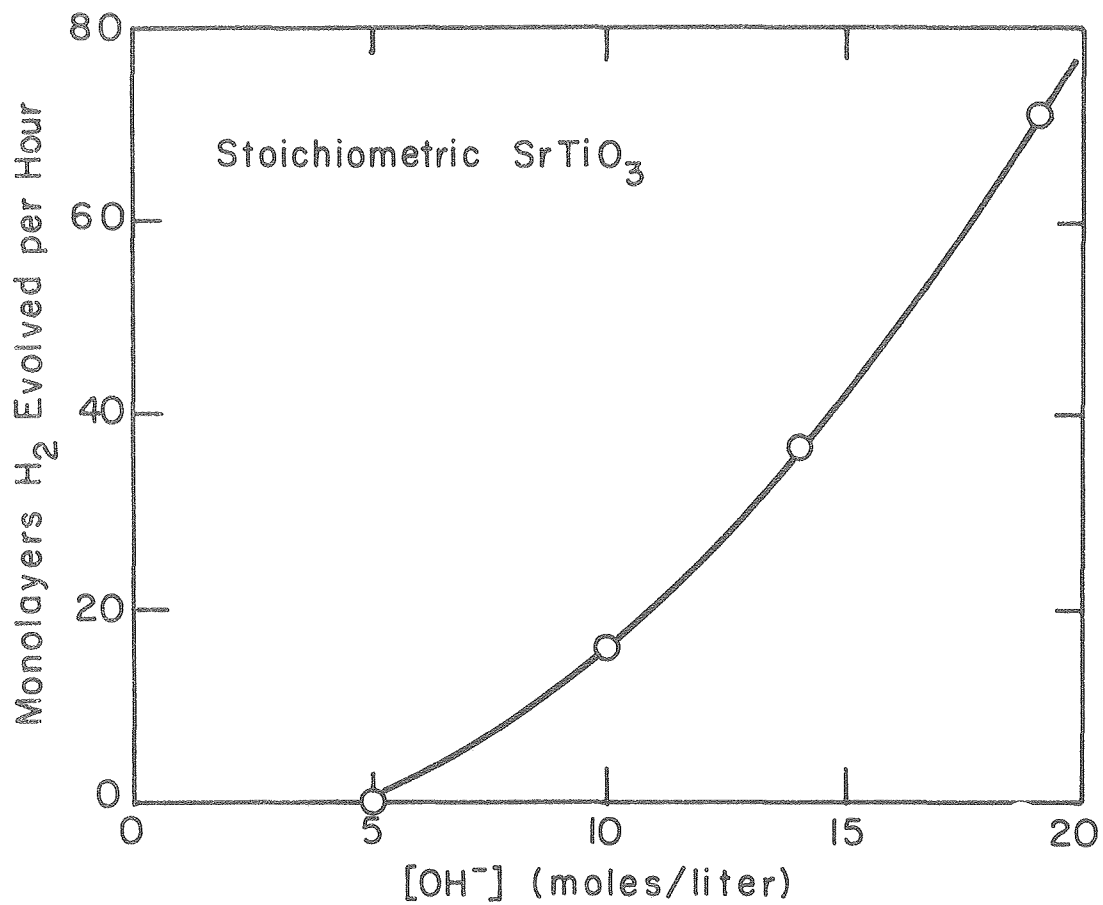
XBL7910-7181

Fig.6



XBL 7910-7182

Fig.7



XBL 7910-7183

Fig.8